

Supporting Information for
**Evaluation of pH at Charged Lipid/Water Interfaces by
Heterodyne-Detected Electronic Sum Frequency Generation**

Achintya Kundu¹, Shoichi Yamaguchi¹, and Tahei Tahara^{1,2*}

¹Molecular Spectroscopy Laboratory, RIKEN, Wako, Saitama 351-0198, Japan

²Ultrafast Spectroscopy Research Team, RIKEN Center for Advanced Photonics (RAP), Wako, Saitama
351-0198, Japan

1. Materials

4-heptadecyl-7-hydroxycoumarin (HHC) was purchased from Fluka and used as received. The cationic lipid, 1,2-dipalmitoyl-3-trimethylammonium-propane (DPTAP) and the anionic lipid, 1,2-dipalmitoyl-sn-glycero-3-phosphoglycerol (DPPG) were purchased as lyophilized powders from Avanti Polar Lipids. Chloroform (99.7%, GC 149 grade) was purchased from Kanto Chemical Co. and used as obtained. Sodium hydroxide and hydrochloric acid was purchased from Wako and used as received. Purified water (Millipore, 18.2 M Ω cm resistivity) was used. Sodium chloride was purchased from Junsei Chemical Co. and used as received. 1,4-dioxane was purchased from Nacalai Tesque and used as received. The surface pressure was measured with a commercial surface tension meter (Kibron, Inc., Helsinki, Finland). Heterodyne-detected electronic sum frequency generation (HD-ESFG) measurements were done in liquid condensed (LC) phase for all the lipids. The bulk pH was regulated by the concentrations of sodium hydroxide and hydrochloric acid, and it was measured using a commercial pH meter (Horiba, B-212). All the experiments were done at 296 ± 2 K.

2. HD-ESFG

The experimental details of HD-ESFG spectroscopy were described previously.¹ In brief, a Ti:sapphire regenerative amplifier system (Spectra Physics, Spitfire Pro XP, 120 fs, 1 kHz, 3.5 mJ) was used as the light source. One portion of the amplifier output was used as a narrow-band ω_1 pulse (795 nm), and the other was focused into water to generate a broad-band ω_2 pulse (540 nm \sim 1.2 μ m). The ω_1 and ω_2 pulses were noncollinearly focused onto the same spot at the lipid/water interface. When the ω_1 and ω_2 pulses were temporally and spatially overlapped, the sum frequency ($\omega_1 + \omega_2$) was generated at the lipid/water

interface. The ω_1 , ω_2 , and $\omega_1 + \omega_2$ pulses were again focused by a spherical concave mirror onto a GaAs (110) surface to generate the sum frequency of ω_1 and ω_2 , once more, which acted as a local oscillator field. A fused-silica glass plate with 1-mm thickness was placed between the sample and concave mirror. The glass substrate delayed the $\omega_1 + \omega_2$ pulse relative to the reflected ω_1 pulse by 170 fs, due to the frequency-dependent difference in the group velocity. This delay resulted in the time difference between the $\omega_1 + \omega_2$ pulse generated from the sample and that from GaAs. The $\omega_1 + \omega_2$ pulse from the sample and that from GaAs propagated collinearly and sequentially through an analyzing polarizer and entered a polychromator. After being spectrally dispersed, the $\omega_1 + \omega_2$ sum frequency light was detected by a multichannel detector (Roper Scientific, Spec-10:2KBUV). Interference fringes between the two $\omega_1 + \omega_2$ pulses were superimposed on the detected spectra. Fourier analysis of the interference fringes yielded the complex $\chi^{(2)}$ spectra of the pH indicator at the lipid/water interfaces. The $\omega_1 + \omega_2$, ω_1 , and ω_2 pulses were s-, p-, and s-polarized, respectively, which is conventionally abbreviated as the SPS polarization combination.

3. Fitting analysis to obtain the dissociation degree

The $\chi^{(2)}$ spectra shown in Fig. 2 in the main text can be analyzed to obtain the bulk-pH dependence of the dissociation degree of the pH indicator at the DPTAP/water interface. The dissociation degree is defined as $[A^-] / ([HA] + [A^-])^{-1}$, where HA and A^- stand for the acid and conjugate base of the pH indicator, respectively.² The fraction of HA, $f_{HA}(\text{pH})$, and that of A^- , $f_A(\text{pH})$, are the function of the bulk pH, and they are expressed as follows:

$$f_{HA}(\text{pH}) = \frac{[HA]}{[HA] + [A^-]} = \frac{1}{1 + 10^{\text{pH} - x}} \quad , \quad (1)$$

$$f_A(\text{pH}) = \frac{[A^-]}{[HA] + [A^-]} = \frac{10^{\text{pH} - x}}{1 + 10^{\text{pH} - x}} \quad . \quad (2)$$

Note that the ‘pH’ here is the bulk pH. In these formulas, x is the bulk pH at which $f_{HA}(\text{pH})$ and $f_A(\text{pH})$ are equal. The dissociation degree is given by $f_A(\text{pH})$. An experimentally-obtained spectrum at $\text{pH} = \text{pH}^i$ is represented by $S^i(\lambda)$, where i ($=1, 2, \dots, N$) stands for a data index, and λ represents wavelength. $S^i(\lambda)$ corresponds to each spectrum in Fig. 2. The spectrum of HA, $S_{HA}(\lambda)$, and that of A^- , $S_A(\lambda)$, are unknown, but they can be expressed by a linear combination of two $S^i(\lambda)$'s, for example, $S^1(\lambda)$ and $S^N(\lambda)$:

$$S_{\text{HA}}(\lambda) = c_{\text{HA}}^1 S^1(\lambda) + c_{\text{HA}}^N S^N(\lambda) , \quad (3)$$

$$S_{\text{A}}(\lambda) = c_{\text{A}}^1 S^1(\lambda) + c_{\text{A}}^N S^N(\lambda) , \quad (4)$$

where c_{HA}^1 , c_{HA}^N , c_{A}^1 , c_{A}^N are unknown coefficients of the linear combinations. Then, $S^i(\lambda)$ for any i can be expressed as follows:

$$S^i(\lambda) = f_{\text{HA}}(\text{pH}^i) S_{\text{HA}}(\lambda) + f_{\text{A}}(\text{pH}^i) S_{\text{A}}(\lambda) . \quad (5)$$

Eq 5 was used as a fitting function for each spectrum in Fig. 2 in the main text, with x , c_{HA}^1 , c_{HA}^N , c_{A}^1 , c_{A}^N treated as global fitting parameters. Supplementary Figure S1 shows that fitting curves are in good agreement with the experimentally-obtained spectra. The x value at the DPTAP/water interface was determined to be 7.8 directly through this fitting analysis. The $\chi^{(2)}$ spectra of HA and A^- ($S_{\text{HA}}(\lambda)$ and $S_{\text{A}}(\lambda)$) at the DPTAP/water interface were obtained by this fitting analysis, as shown in Supplementary Figures S2a and S2b. The peak wavelength of the $\text{Im}[\chi^{(2)}]$ spectrum of A^- was determined to be 377 nm by a Gaussian fitting to the spectrum obtained with this procedure.

Similarly, Eq 5 was used as a fitting function for each spectrum in Fig. 3 in the main text, with x , c_{HA}^1 , c_{HA}^N , c_{A}^1 , c_{A}^N treated as global fitting parameters. Supplementary Figure S3 shows that fitting curves are in good agreement with the experimentally-obtained spectra. The x value at the DPPG/water interface was determined to be 10.7. Supplementary Figures S4a and 4b show the $\chi^{(2)}$ spectra of HA and A^- at the DPPG/water interface. The peak wavelength of the $\text{Im}[\chi^{(2)}]$ spectrum of A^- was determined to be 366 nm by a Gaussian fitting to the spectrum obtained with this procedure.

4. Salt concentration dependence of the UV-visible absorption spectrum of the pH indicator

To confirm that the pH indicator is not charge sensitive, we performed UV-visible absorption measurements of 4-methyl-7-hydroxycoumarin (MHC; Supplementary Figure S5a) in two different dielectric environments with different salt concentrations. MHC was purchased from Aldrich and used as received. We used MHC, because it has the same chromophoric structure as 4-heptadecyl-7-hydroxycoumarin, and it is very well soluble in bulk water. Supplementary Figure S5b shows the absorption spectra of the conjugate base of MHC (A^-) in bulk water ($\epsilon = 77.8$) with different NaCl concentrations. Supplementary Figure

S5c shows the absorption spectra of A⁻ in a water/1,4-dioxane mixture ($\epsilon = 27.5$) with different NaCl concentrations. These spectra clearly demonstrate that the peak wavelength of the A⁻ absorption spectrum does not change with the salt concentration at all. This indicates that the present pH indicator is not charge sensitive.

5. Effect of aligned charges on the electronic spectrum of the pH indicator

It is experimentally proved in the section 4 that the pH indicator is not charge sensitive. However, the effect of aligned charges is not taken into account in the section 4, because the charges in the bulk salt solution are not aligned but isotropically distributed. In this section 5, the effect of the aligned charges at the lipid/water interfaces is estimated.

The most important effect of the aligned charges on the electronic spectrum of the pH indicator is the Stark effect. The peak energy shift induced by the Stark effect is given by the interaction between the permanent dipole moment and the static electric field:³

$$\Delta\epsilon_p = -(\mathbf{m}_e - \mathbf{m}_g) \cdot \mathbf{E}, \quad (6)$$

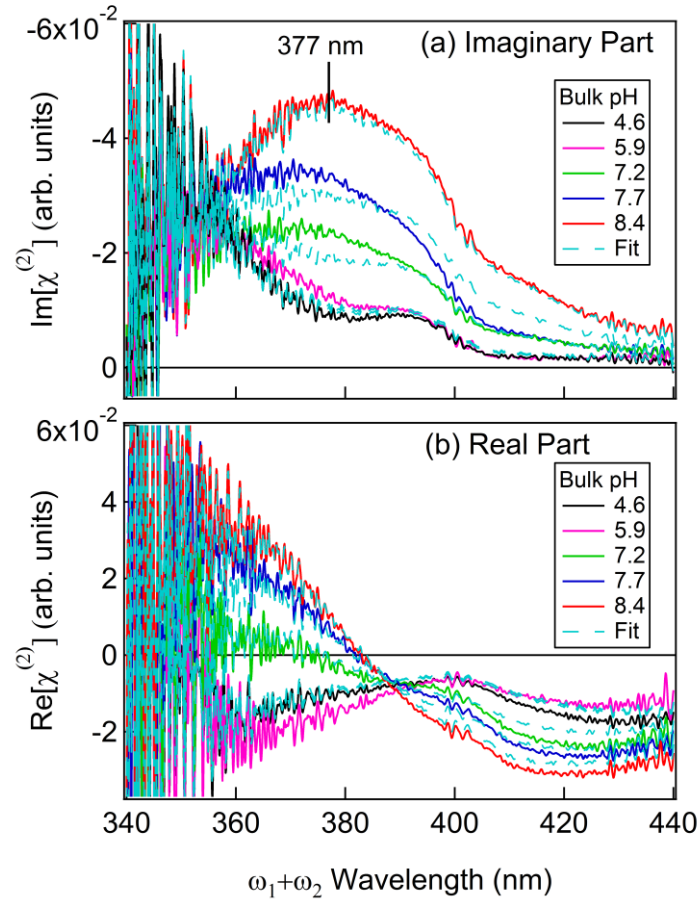
where $\Delta\epsilon_p$ is the peak energy shift, \mathbf{m}_e and \mathbf{m}_g are the permanent dipole moments of the chromophore of the pH indicator in the electronically excited and ground states, respectively, and \mathbf{E} represents the static electric field generated by the aligned charges. For the present estimation, the magnitude of $\mathbf{m}_e - \mathbf{m}_g$ is assumed to be 1.1×10^{-29} C m which is given by the theoretical calculation of a coumarin molecule.⁴ The aligned charges are assumed to form a simple electric double layer with the charge density of 0.08 C m⁻² which is given by the molecular dynamics simulation of lipid membranes.⁵ Then, the magnitude of \mathbf{E} is calculated to be 1.1×10^8 V m⁻¹ with use of the relative dielectric constant of water (78.5). The peak energy shift $\Delta\epsilon_p$ depends on the angle θ between the two vectors $\mathbf{m}_e - \mathbf{m}_g$ and \mathbf{E} . Supplementary Table I shows the shift of the peak wavelength of the pH indicator (361 nm) which is converted from $\Delta\epsilon_p$ with different θ values. It is clear that the peak wavelength shift by the Stark effect is always less than 1 nm, and it is much smaller than the solvatochromic shift discussed in the present study.

Supplementary Table I. Peak wavelength shift of the electronic spectrum at different θ .

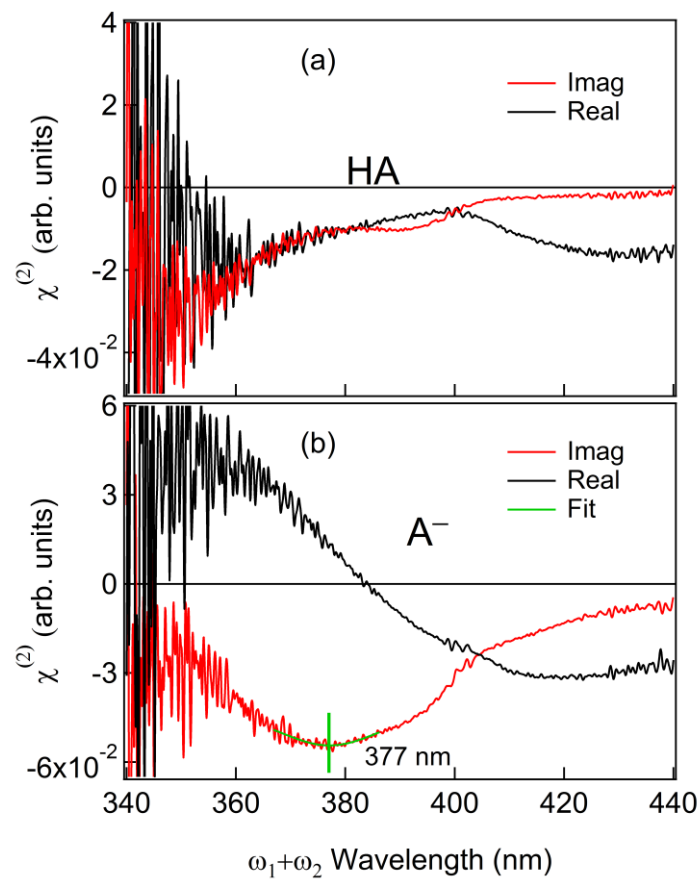
θ	Peak shift (nm)
0°	0.7
20°	0.6
40°	0.5
60°	0.3
80°	0.04

References

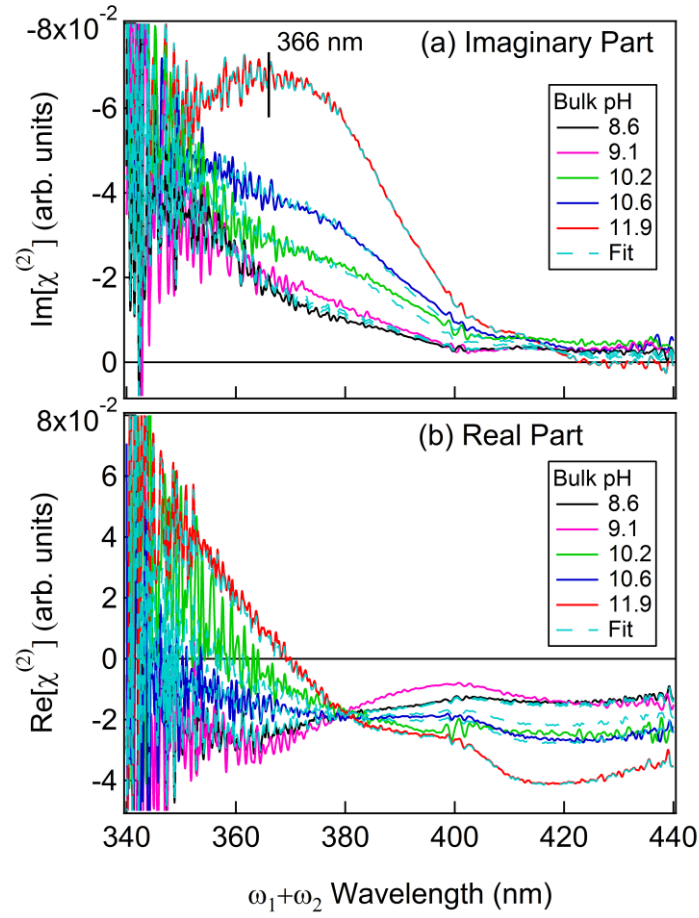
- (1) Yamaguchi, S.; Tahara, T. Heterodyne-Detected Electronic Sum Frequency Generation: "Up" versus "down" Alignment of Interfacial Molecules. *J. Chem. Phys.* **2008**, *129*, 101102-101108.
- (2) Yamaguchi, S.; Kundu, A.; Sen, P.; Tahara, T. Communication: Quantitative Estimate of the Water Surface pH Using Heterodyne-Detected Electronic Sum Frequency Generation. *J. Chem. Phys.* **2012**, *137*, 151101-151105.
- (3) Yamasaki, K.; Okada, O.; Inami, K.; Oka, K.; Kotani, M.; Yamada, H. Gallium Phthalocyanines: Structure Analysis and Electroabsorption Study. *J. Phys. Chem. B* **1997**, *101*, 13-19.
- (4) Nemkovich, N. A.; Reis, H.; Baumann, W. Ground and excited state dipole moments of coumarin laser dyes: Investigation by electro-optical absorption and emission methods. *J. Lumin* **1997**, *71*, 255-263.
- (5) Gurtovenko, A. A.; Miettinen, M.; Karttunen, M.; Vattulainen, I. Effect of Monovalent Salt on Cationic Lipid Membranes As Revealed by Molecular Dynamics Simulations. *J. Phys. Chem. B* **2005**, *109*, 21126-21134.



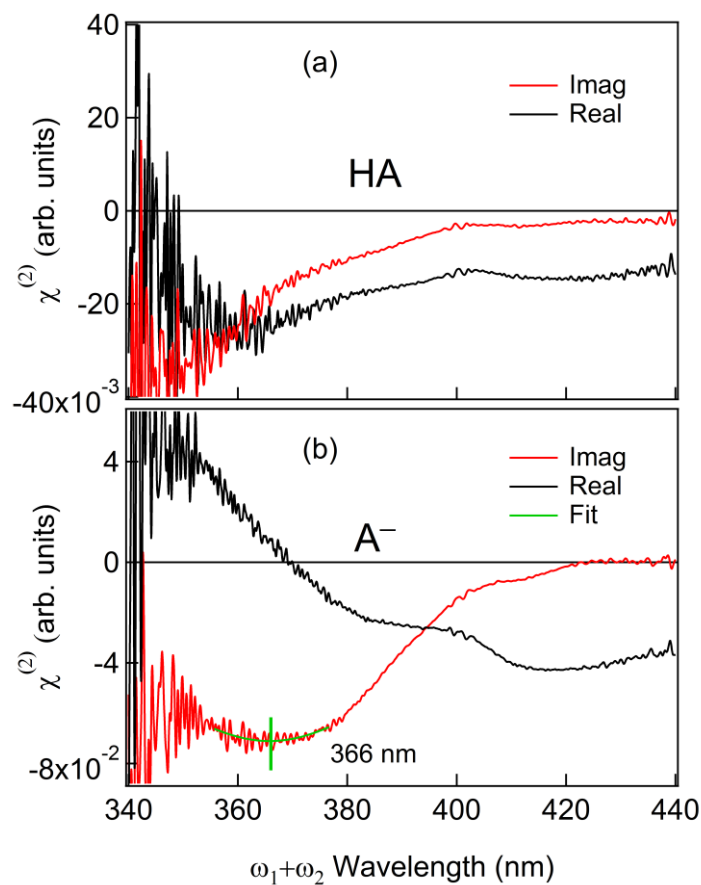
Supplementary Figure S1. Interface-selective electronic spectra of the pH indicator at the DPTAP/water interface. Black, pink, green, blue, and red solid lines represent spectra at the bulk pH 4.6, 5.9, 7.2, 7.7, and 8.4, respectively. The imaginary and real parts of $\chi^{(2)}$ are shown in (a) and (b), respectively. Cyan broken lines represent fits based on Eq 5.



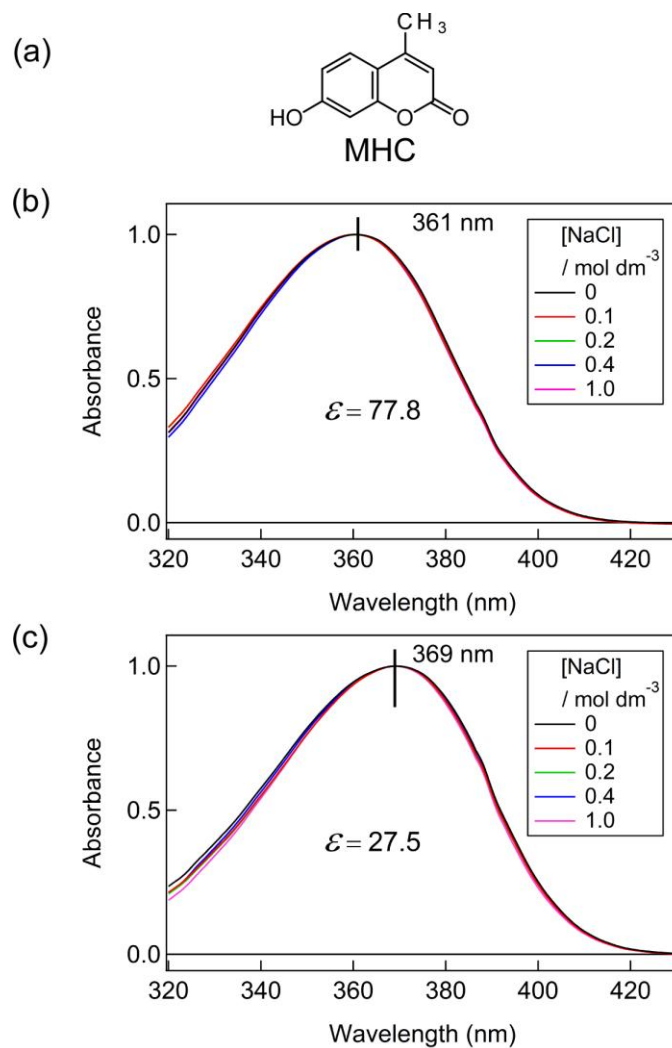
Supplementary Figure S2. Interface-selective electronic spectra of the acid (a) and the conjugate base (b) of the pH indicator at the DPTAP/water interface. Red and black lines are the $\text{Im}[\chi^{(2)}]$ and $\text{Re}[\chi^{(2)}]$, respectively. The green solid line represents a fit with a Gaussian function.



Supplementary Figure S3. Interface-selective electronic spectra of the pH indicator at the DPPG/water interface. Black, pink, green, blue, and red solid lines represent spectra at the bulk pH 8.6, 9.1, 10.2, 10.6, and 11.9, respectively. The imaginary and real parts of $\chi^{(2)}$ are shown in (a) and (b), respectively. Cyan broken lines represent fits based on Eq 5.



Supplementary Figure S4. Interface-selective electronic spectra of the acid (a) and the conjugate base (b) of the pH indicator at the DPPG/water interface. Red and black lines are the $\text{Im}[\chi^{(2)}]$ and $\text{Re}[\chi^{(2)}]$, respectively. The green solid line represents a fit with a Gaussian function.



Supplementary Figure S5. (a) Molecular structure of 4-methyl-7-hydroxycoumarin. (b) Absorption spectra of the conjugate base of MHC in water with different salt concentrations. (c) Absorption spectra of the conjugate base of MHC in water/1,4-dioxane mixture with different salt concentrations.